# Dielectric strength, optical absorption, and deep ultraviolet detectors of hexagonal boron nitride epilayers

J. Li, S. Majety, R. Dahal, W. P. Zhao, J. Y. Lin et al.

## Related Articles

## Additional information on Appl. Phys. Lett.

# Dielectric strength, optical absorption, and deep ultraviolet detectors of hexagonal boron nitride epilayers

J. Li, S. Majety, R. Dahal, W. P. Zhao, J. Y. Lin, and H. X. Jiang[a)]
*Department of Electrical and Computer Engineering, Texas Tech University, Lubbock, Texas 79409, USA*

Hexagonal boron nitride (hBN) epilayers have been synthesized by metal organic chemical vapor deposition and their dielectric strength, optical absorption, and potential as a deep ultraviolet (DUV) detector material have been studied. Based on the graphene optical absorption concept, the estimated band-edge absorption coefficient of hBN is about $7 \times 10^5$/cm, which is more than 3 times higher than the value for wurtzite AlN ($\sim 2 \times 10^5$ /cm). The dielectric strength of hBN epilayers exceeds that of AlN and is greater than 4.4 MV/cm based on the measured result for an hBN epilayer released from the host sapphire substrate. The hBN epilayer based DUV detectors exhibit a sharp cut-off wavelength around 230 nm, which coincides with the band-edge photoluminescence emission peak and virtually no responses in the long wavelengths. Based on the present study, we have identified several advantageous features of hBN DUV photodetectors: (1) low long wavelength response or high DUV to visible rejection ratio; (2) requiring very thin active layers due to high optical absorption; (3) high dielectric strength and chemical inertness and resistance to oxidation and therefore suitable for applications in extreme conditions; (4) high prospects of achieving flexible devices; and (5) possible integration with graphene optoelectronics due to their similar structures and lattice constants. © *2012 American Institute of Physics.*
[http://dx.doi.org/10.1063/1.4764533]

Hexagonal boron nitride (hBN) possesses extraordinary physical properties including high-temperature stability, large thermal conductivity, high chemical stability and high corrosion resistance, large negative electron affinity, low dielectric constant, large energy band gap ($E_g \sim 6$ eV), and large neutron capture cross section.[1–4] Due to its layered structure and similar lattice constants to graphene, hBN is also highly suitable for use as a template in graphene electronics and as a gate dielectric layer[5–9] and provides an ideal platform to study fundamental properties of layer-structured materials. Moreover, lasing action in deep ultraviolet (DUV) region ($\sim$225 nm) by electron beam pumping was demonstrated in millimeter size hBN bulk crystals,[10] raising its promise for realizing chip-scale DUV light sources. In principle, hBN should also be very promising for DUV detector applications. However, so far, bulk crystal growth techniques can only produce a sample size around 1 mm,[10–14] limiting the prospects for implementing hBN as an active device material. Most recently, we have demonstrated that the synthesis of wafer-scale semiconducting hBN epitaxial layers with high crystalline and optical qualities is possible with metal organic chemical vapor deposition (MOCVD),[4,15–17] thereby providing an opportunity to explore hBN as an active material for DUV optoelectronic device applications. Active DUV ($\lambda < 280$ nm) optoelectronic devices are highly useful in areas such as probing intrinsic fluorescence in a protein, equipment/personnel decontamination, photocatalysis, and UV astronomy and UV metrology. In this work, we synthesized hBN epilayers by MOCVD and studied their dielectric strength, optical absorption, and potential as a deep UV detector material.

Hexagonal BN epitaxial layers were grown by MOCVD on sapphire substrates. Triethylboron (TEB) and ammonia ($NH_3$) were used as B and N precursors, respectively, and $H_2$ was used as the carrier gas. Due to the crystal structure mismatch between sapphire and hBN, prior to epilayer growth, a 20 nm BN buffer layer was first deposited on sapphire substrate at 800 °C. Similar to the case in the conventional III-nitride epitaxial growth, the functions of this buffer layer include providing strain relieve from lattice mismatch between the substrate and the subsequent hBN epilayer. Furthermore, it was found that the use of this buffer layer enhances significantly the adhesion of the hBN epilayer to the substrate. Though we are certain that this buffer layer is of amorphous nature, its properties have not yet been studied in detail as hBN epilayers are in the early development stage. The typical hBN epilayer growth temperature was about 1300 °C. A high quality and well characterized AlN epilayer (1 $\mu$m thick) grown on c-plane sapphire by MOCVD[18–20] was used as a reference for comparison studies since wurtzite AlN has a similar band gap as hBN. X-ray diffraction (XRD) $\theta$-2$\theta$ scan for an hBN epilayer of 1 $\mu$m in thickness shown in Fig. 1(a) revealed a *c*-lattice constant $\sim$6.67 Å, which closely matches to the bulk *c*-lattice constant of hBN (c = 6.66 Å),[1,21] affirming that BN films are of single hexagonal phase. However, the XRD intensity of the (0002) peak of hBN is about 30 times lower than that of AlN epilayer with the same thickness. The XRD rocking curve of the (0002) reflection has a full width at half maximum (FWHM) of $\sim$400 arcsec for the hBN,[15] which is a dramatic improvement over previously reported values for hBN films (1.5°–0.7°),[22] but is 5–8 times broader than the typical FWHM of high quality AlN epilayers.[20] The results are an indicative of the fact that the development of epitaxial layers of hBN is in its early stage.
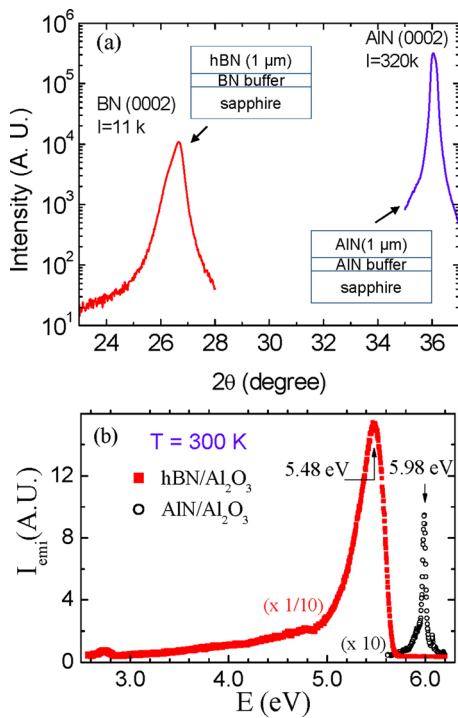
a)hx.jiang@ttu.edu.

FIG. 1. (a) XRD $\theta$–$2\theta$ scans of 1 $\mu$m thick hBN and wurtzite AlN epilayers grown on sapphire substrate by MOCVD. The inset shows the schematics of hBN and AlN epilayers. The relative XRD intensities are indicated for hBN and AlN. (b) Room temperature (300 K) PL spectra of hBN and AlN epilayers grown on sapphire substrate by MOCVD.

Figure 1(b) shows the comparison of photoluminescence (PL) spectra of our hBN and AlN epilayers measured side-by-side at room temperature. Despite the fact that the crystalline quality of AlN is superior over hBN, the band-edge PL emission from hBN is more than two orders of magnitude higher than that of AlN, which is considered to be a highly efficient emission material and is the current default choice for DUV device implementation. One of the major reasons for the high band-edge emission efficiency in hBN is thought to be due to its layered structure.[23] Recent theoretical studies have also suggested that an efficient band-edge emission is expected from hBN due to its graphite like layered structure and small lattice constant in the c-plane.[24,25] The layer structured hBN provides a natural 2D system which can result in an increase in the exciton binding energy and oscillator strength over the 3D systems such as AlN.[26] Another factor that may account for this efficient band-edge emission in hBN is the high band-edge optical absorption coefficient.[3]

The previously measured band-edge optical absorption coefficient ($\alpha$) of hBN is unusually high ($\sim 7.5 \times 10^5$ cm$^{-1}$)[3] and is more than 3 times higher than that of AlN ($\sim 2 \times 10^5$ cm$^{-1}$).[27,28] To understand this unique property, we write the optical absorption (I) as

$$I = I_0(1 - e^{-t/\lambda}), \tag{1}$$

where $\lambda$ is the optical absorption length. On the other hand, we can rewrite Eq. (1) as follows:

$$I/I_0 \approx (t/\lambda), \quad \text{for} \quad (t/\lambda) \ll 1. \tag{2}$$

One important and interesting feature of graphene is that its absorption is determined by fundamental constants following

$\pi e^2/\hbar c = \pi\alpha = 2.3\%$, where $\alpha = e^2/\hbar c$ is the fine structure constant, which describes the coupling between light and relativistic electrons.[29] If we assume the same holds for hBN, we then have the optical absorption of hBN = 2.3% per layer (3.33 Å). This means that $I/I_0 = (t/\lambda) = 0.023$ with t = 3.33 Å. This gives

$$\lambda = t/0.023 = 3.33\text{Å}/0.023 = 144.8\text{Å},$$
$$\alpha = 1/\lambda = 1/144.8\text{Å} = 6.9 \times 10^{-3}/\text{Å} \approx 7 \times 10^5/\text{cm}.$$

The estimated value of the band-edge optical absorption coefficient ($\alpha$) based on the optical absorption concept from graphene agrees exceptionally well with the previously measured value of about $7.5 \times 10^5$ cm$^{-1}$.[3] This means that only a very thin layer of hBN with approximately 70 nm ($\sim 5\lambda$) in thickness will absorb all incoming photons. This together with its inherent nature of layered structure makes hBN an exceptionally efficient emitter. However, its potential as a DUV photodetector material has not yet been explored.

As a natural consequence of the crystal structure of hBN, very different bonding, i.e., strong covalent bonding within the basal planes and weak bonding between planes, leads to high anisotropy in most basic properties of hBN. Therefore, it is expected that the electrical conductivity is much higher within the planes than in the direction perpendicular to them (c-direction). By taking the high optical absorption and anisotropy into consideration, we exploited a micro-strip geometry for the photodetector fabrication. We expect the design to improve the collection of photoexcited carriers and at the same time to more effectively utilize the lateral transport properties within the basal planes in hBN. The inset of Fig. 1(a) shows the schematic of the device layer structure employed in this study. The metal-semiconductor-metal (MSM) detector consists of micro-strip interdigital fingers (4 $\mu$m/4 $\mu$m of width/spacing) of Schottky contact formed by a bilayer of Ni/Au (5 nm/5 nm). Micro-strips were formed by inductively coupled plasma dry etching with $\sim 0.2$ $\mu$m etching depth. For device characterization, bonding pads were then formed by depositing an Au (200 nm) layer. For the steady current response measurements, an electrometer (Keithley 617) and a source-meter (Keithley 2410) are connected in series. A broad spectral light source in conjunction with a monochromator was used as an excitation source covering wavelength range from 800 to 180 nm.

The typical I-V characteristics of hBN epilayer based MSM detectors are shown in Fig. 2(a). The devices exhibit low dark current and current density of $\sim 200$ pA and $10^{-10}$ A/cm$^2$ at a bias voltage of 100 V, respectively. The relative spectral responses have been measured at different bias voltages ($V_b$) and an example is shown in Fig. 2(b) for $V_b = 30$ V. These hBN MSM detectors exhibit a peak responsivity of 220 nm, a sharp cut-off wavelength around 230 nm, which corresponds well with the band-edge PL emission peak at 5.48 eV (or 227 nm). An outstanding feature observed from hBN photodetectors is that there are virtually no detectable responses in the long wavelengths measured up to 800 nm. However, the observed DUV to visible rejection ratio in hBN MSM detectors is still 2–3 orders of magnitude lower than that of AlN based detectors.[30,31] This corroborates the fact that the crystalline quality of hBN is not yet as good as those
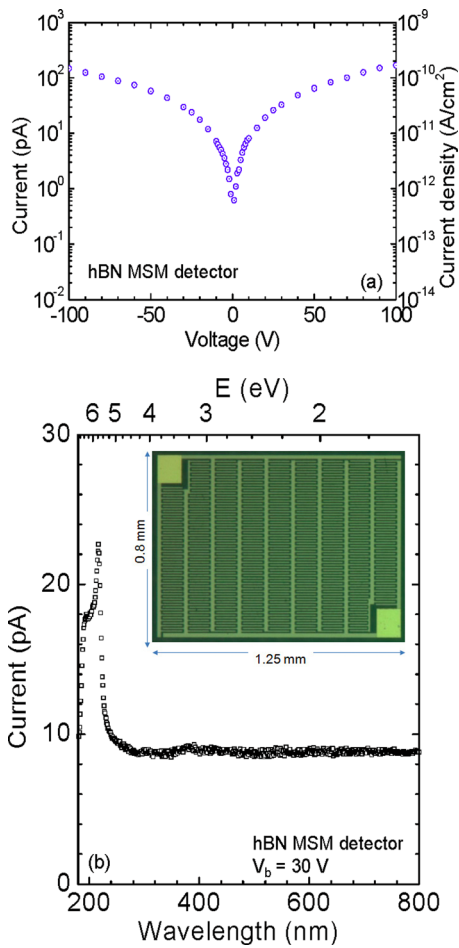
FIG. 2. (a) In plane I–V characteristics of a hBN MSM photodetector fabricated from the layer structure shown in the inset of Fig. 1(a). (b) The relative spectral response of hBN MSM detector measured at $V_b = 30$ V. The inset is a microscope image of the hBN MSM photodetector with a device size of 1.25 mm $\times$ 0.8 mm and 4 $\mu$m/4 $\mu$m finger width/spacing used for the measurements.
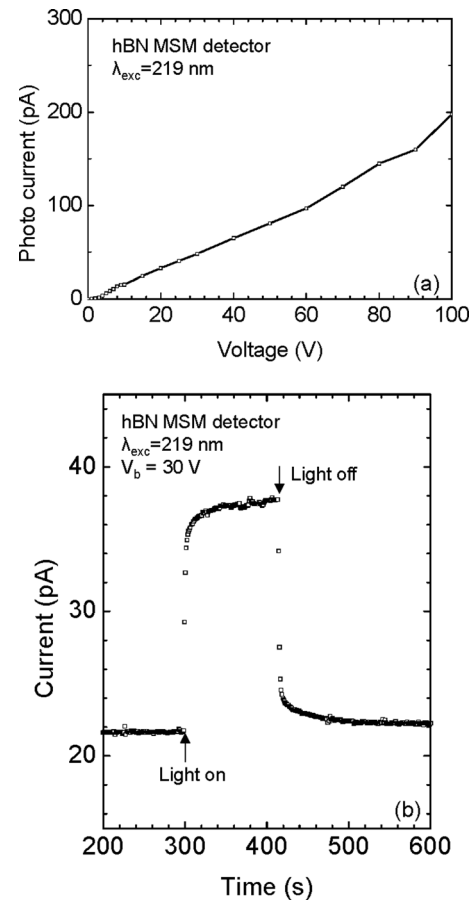


FIG. 3. (a) The relative photoresponsivity of hBN MSM detector as a function of the applied bias voltage and (b) photocurrent decay kinetics of hBN MSM detector measured at room temperature for $\lambda_{exc} = 219$ nm.

of high quality AlN, as confirmed by the XRD results shown in Fig. 1(a). The relative responsivity increases almost linearly with the bias voltage, as illustrated in Fig. 3(a), which suggests that hBN MSM detector has a gain. This may be attributed to the presence of dislocations or impurities in the epilayers. However, the photocurrent kinetics of hBN MSM detector measured at room temperature shown in Fig. 3(b) exhibit no persistent photoconductivity (PPC) effects. The presence of PPC is generally regarded as an indicative of existence of deep metastable charge trapping centers or local potential fluctuations caused by material inhomogeneity.[32,33]

One other important parameter of a semiconductor for detector applications is the dielectric strength or the breakdown field ($E_B$) in the *c*-direction. A previous study has obtained $E_B = 7.94$ MV/cm for ultrathin hBN layers mechanically exfoliated from powder crystals.[34] Since our hBN epilayers were grown on sapphire substrates, it was necessary to release epilayers from the host sapphire substrate in order to conduct $E_B$ measurements. We first deposited a bilayer of Ni/Au Schottky contact on a 1.8 $\mu$m thick hBN epilayer and then coated the Ni/Au Schottky contact with Ag past. Next, we glued the structure to a second sapphire substrate and then released the epilayer from the host sapphire substrate by mechanical force.[35] Finally, another bilayer of Ni/Au Schottky

contact was deposited on the back side of the released hBN epilayer. A schematic of the device structure for $E_B$ measurements is shown in Fig. 4(a).

Figure 4(b) shows the I-V characteristics of the released hBN epilayer in the *c*-direction (out-of-plane), which indicate that the breakdown occurs at around 800 V. This translates to $E_B \sim 4.4$ MV/cm, which is lower than that obtained from ultrathin hBN layers exfoliated from powder crystals having a cross section area in micron scale. Not only our released hBN epilayer used for $E_B$ measurement has a large cross section area of $\sim 4$ mm$^2$ but also hBN epitaxial layers are grown on foreign substrate and are not dislocation free. It was demonstrated previously in AlN epilayer detectors that $E_B$ increases linearly with a decrease in the device area (A), since the number of dislocations decreases linearly with a decrease in A.[31] $E_B$ for dislocation-free AlN epilayers was obtained by extrapolating A to zero ($\sim 4.1$ MV/cm).[31] Moreover, the backside of the released hBN epilayer contains a 20 nm low temperature buffer layer of amorphous nature, which also reduced the measured value of $E_B$ of hBN. Our results shown in Fig. 4(b) clearly indicate that hBN epilayers have a higher $E_B$ than AlN epilayers. If we assume ultrathin hBN layers exfoliated from powder crystals are dislocation free, then the value of 7.94 MV/cm (Ref. 34) may represent the $E_B$ value of intrinsic hBN. Our results thus suggest that the device performance can be improved by improving
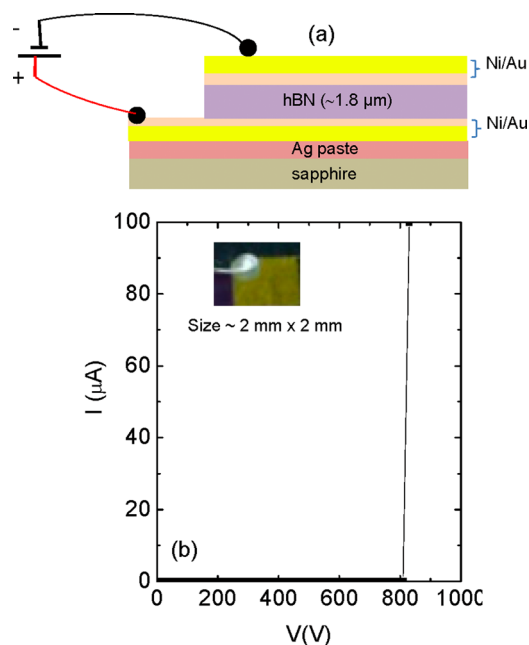
FIG. 4. (a) Schematic of an hBN epilayer released from the host sapphire substrate for breakdown field ($E_B$) measurement. The structure has a cross section area of about $\sim$4 mm$^2$. (b) Out-of-plane (vertical) I–V characteristics of a released hBN epilayer. The inset is a microscope image of the device employed for $E_B$ measurement.

material quality, mainly reducing dislocation density, and optimizing the device size and geometry.

In summary, we have synthesized high quality hBN epilayers by MOCVD and explored them as DUV detector materials. Based on the graphene optical absorption concept, the estimated band-edge absorption coefficient of hBN is about $7 \times 10^5$/cm, which is more than 3 times higher than the value for AlN ($\sim 2 \times 10^5$ /cm). The dielectric strength of hBN epilayers exceeds that of AlN epilayers and is greater than 4.4 MV/cm based on the measured result for an hBN epilayer released from the host sapphire substrate. The hBN epilayer based DUV detectors have a sharp cut-off wavelength around 230 nm, which coincides with the band-edge PL emission peak and showed virtually no response in the long wavelengths measured up to 800 nm. Currently, our understanding of hBN epilayer growth and properties is still in the very early stage compared to the status of AlN epilayers. Much improvement is anticipated for hBN, which ultimately will lead to functional practical devices.

[1]S. L. Rumyantsev, M. E. Levinshtein, A. D. Jackson, S. N. Mohammmad, G. L. Harris, M. G. Spencer, and M. S. Shur, in *Properties of Advanced Semiconductor Materials GaN, AlN, InN, BN, SiC, SiGe*, edited by M. E. Levinshtein, S. L. Rumyantsev, and M. S. Shur (John Wiley & Sons, Inc., New York, 2001), pp. 67–92.

[2]Y. Kubota, K. Watanabe, O. Tsuda, and T. Taniguchi, Science **317**, 932 (2007).

[3]T. Sugino, K. Tanioka, S. Kawasaki, and J. Shirafuji, Jpn. J. Appl. Phys., Part 2 **36**, L463 (1997).

[4]J. Li, R. Dahal, S. Majety, J. Y. Lin, and H. X. Jiang, Nucl. Instrum. Methods Phys. Res. A **654**, 417 (2011).

[5]L. Song, L. Ci, H. Lu, P. B. Sorokin, C. Jin, J. Ni, A. G. Kvashnin, D. G. Kvashnin, J. Lou, B. I. Yakobson, and P. M. Ajayan, Nano Lett. **10**, 3209 (2010).

[6]R. V. Gorbachev, I. Riaz, R. R. Nair, R. Jalil, L. Britnell, B. D. Belle, E. W. Hill, K. S. Novoselov, K. Watanabe, T. Taniguchi, A. K. Geim, and P. Blake, Small **7**, 465 (2011).

[7]Y. Shi, C. Hamsen, X. Jia, K. K. Kim, A. Reina, M. Hofmann, A. L. Hsu, K. Zhang, H. Li, Zy. Juang, M. S. Dresselhaus, L. J. Li, and J. Kong, Nano Lett. **10**, 4134 (2010).

[8]N. Alem, R. Erni, C. Kisielowski, M. D. Rossell, W. Gannett, and A. Zettl, Phys. Rev. B **80**, 155425 (2009).

[9]C. R. Dean, A. F. Young, I. Meric, C. Lee, L. Wang, S. Sorgenfrei, K. Watanabe, T. Taniguchi, P. Kim, K. L. Shepard, and J. Hone, Nat. Nanotechnol. **5**, 722 (2010).

[10]K. Watanabe, T. Taniguchi, and H. Kanda, Nature Photon. **3**, 591 (2009).

[11]T. Taniguchi and K. Watanabe, J. Cryst. Growth **303**, 525 (2007).

[12]K. Watanabe, T. Taniguchi, T. Kuroda, O. Tsuda, and H. Kanda, Diamond Relat. Mater. **17**, 830 (2008).

[13]K. Watanabe and T. Tanniguchi, Phys. Rev. B **79**, 193104 (2009).

[14]K. Watanabe and T. Taniguchi, Int. J. Appl. Ceram. Technol. **8**, 977 (2011).

[15]R. Dahal, J. Li, S. Majety, B. N. Pantha, X. K. Cao, J. Y. Lin, and H. X. Jiang, Appl. Phys. Lett. **98**, 211110 (2011).

[16]S. Majety, J. Li, X. K. Cao, R. Dahal, B. N. Pantha, J. Y. Lin, and H. X. Jiang, Appl. Phys. Lett. **100**, 061121 (2012).

[17]S. Majety, X. K. Cao, J. Li, R. Dahal, J. Y. Lin, and H. X. Jiang, Appl. Phys. Lett. **101**, 051110 (2012).

[18]K. B. Nam, J. Li, M. L. Nakarmi, J. Y. Lin, and H. X. Jiang, Appl. Phys. Lett. **82**, 1694 (2003).

[19]J. Li, K. B. Nam, M. L. Nakarmi, J. Y. Lin, H. X. Jiang, P. Carrier, and S.-H. Wei, Appl. Phys. Lett. **83**, 5163 (2003).

[20]B. N. Pantha, R. Dahal, M. L. Nakarmi, N. Nepal, J. Li, J. Y. Lin, H. X. Jiang, Q. S. Paduano, and D. Weyburne, Appl. Phys. Lett. **90**, 241101 (2007).

[21]R. W. Lynch and H. G. Drickamer, J. Chem. Phys. **44**, 181 (1966).

[22]Y. Kobayashi, T. Akasaka, and T. Makimoto, J. Cryst. Growth **310**, 5048 (2008).

[23]B. Huang, H. X. Jiang, X. K. Cao, J. Y. Lin, and S.-H. Wei, Phys. Rev. B **86**, 155202 (2012).

[24]L. Museur, G. Brasse, A. Pierret, S. Maine, B. Attal-Trétout, F. Ducastelle, A. Loiseau, J. Barjon, K. Watanabe, T. Taniguch, and A. Kanaev, Phys. Status Solidi (RRL) **5**, 214 (2011).

[25]B. Arnaud, S. Lebègue, P. Rabiller, and M. Alouani, Phys. Rev. Lett. **96**, 026402 (2006).

[26]P. K. Basu, *Theory of Optical Processes in Semiconductors: Bulk and Microstructures* (Clarendon, Oxford 1997).

[27]P. B. Perry and R. F. Rutz, Appl. Phys. Lett. **33**, 319 (1978).

[28]H. Demiryont, L. R. Thompson, and G. J. Collins, Appl. Opt. **25**, 1311 (1986).

[29]R. R. Nair, P. Blake, A. N. Grigorenko, K. S. Novoselov, T. J. Booth, T. Stauber, N. M. R. Peres, and A. K. Geim, Science **320**, 1308 (2008).

[30]J. Li, Z. Y. Fan, R. Dahal, M. L. Nakarmi, J. Y. Lin, and H. X. Jiang, Appl. Phys. Lett. **89**, 213510 (2006).

[31]R. Dahal, T. M. Al Tahtamouni, J. Y. Lin, and H. X. Jiang, Appl. Phys. Lett. **91**, 243503 (2007).

[32]D. V. Lang, in *Deep Centers in Semiconductors*, edited by S. T. Pantelides (Gordon and Breach, New York, 1986), p. 489.

[33]H. X. Jiang and J. Y. Lin, Phys. Rev. B **40**, 10025 (1989).

[34]G. H. Lee, Y. J. Yu, C. Lee, C. Dean, K. L. Shepard, P. Kim, and J. Hone, Appl. Phys. Lett. **99**, 243114 (2011).

[35]Y. Kobayashi, K. Kumakura, T. Akasaka, and T. Makimoto, Nature **484**, 223 (2012).